17th World Conference on Earthquake Engineering, 17WCEE
Sendai, Japan - September 13th to 18th 2020

RELIABILITY-BASED DESIGN OF FORCE-CONTROLLED COMPONENTS IN ROCKING STEEL BRACED FRAMES

S. Dastmalchi[(1)], H.V. Burton[(2)]

[(1)]*Ph.D. Candidate, Department of Civil and Environmental Engineering, University of California Los Angeles.*
Email:shdstm@ucla.edu
[(2)]*Assistant Professor, Department of Civil and Environmental Engineering, University of California Los Angeles.*
Email:hvburton@seas.ucla.edu

Abstract

Despite their importance, the implication of force-controlled component failure to the overall performance of controlled rocking steel braced frames (CRSBF) has not been examined in prior studies. This paper presents a reliability-based methodology for quantifying the relationship between the response of CRSBF force-controlled components (frame beams, columns and braces) and system-level performance. Structural response simulation of nonlinear models constructed in OpenSees are used to investigate the relationship between the behavior of the CRSBF components and these system-level performance metrics. Vulnerability- and risk-based assessments of the collapse and unsafe placard trigger (UPT) limit states are performed with and without considering the possibility of force-controlled component failure, while varying the ratio between the resistance and load factors ϕ/γ used in their design. The results from a case study using 3-, 6- and 9-story CRSBFs showed that force-controlled component response had a larger influence on collapse safety compared to unsafe placard assignment. Also, for both these limit states, the effect of force-controlled component behavior was lower for taller buildings.

Keywords: controlled rocking braced frame; reliability-based assessment; collapse safety; post-earthquake structural safety

1. Introduction

The controlled rocking steel braced frame (CRSBF) has been the subject of numerous research investigations. Its predictable response and viability as a high-performance structural system has been demonstrated through component- and system-level physical experiments (e.g., [1, 2]). The effect of design parameters such as the aspect ratio, response modification factor and initial post-tensioning force, has also been examined using numerical simulations [e.g. 3, 4]. To enable its implementation in industry building projects, design methodologies and simplified analysis procedures for CRSBFs have been developed (e.g., [5, 6, 7]).

Despite the significant amount of research that has been done on CRSBFs to date, there are several questions related to their design and assessment that have not been addressed. One of the least-studied aspects of CRSBFs is the ability of the braced frame components (beams, columns and braces) to avoid damage when the system experiences moderate-to-severe levels of earthquake shaking. Unlike the fuse and (to a lesser extent) post-tensioning (PT) strands, which are designed and constructed to be replaceable, repairing or replacing elements of the braced frame after an earthquake is a significant undertaking that has strong implications to direct and indirect (due to downtime) economic losses. Therefore, these components are designed using capacity-designed principles with the intent that they remain essentially elastic during moderate-to-severe ground shaking. The research that has been done to date on the braced frame components of CRSBFs has focused on developing methodologies to estimate their design forces and mitigating the effects of higher mode response in taller buildings.

This paper proposes a reliability-based approach to determining the demand and capacity levels used to design the force-controlled components (braced frame elements) of CRSBFs. A key departure from the

abovementioned studies on this topic is that an explicit link between the force-controlled component behavior and system-level performance (collapse and post-earthquake structural safety) is established. This probabilistic relationship directly informs the demand levels and (if necessary) resistance factors used to design the rocking frame elements. First, the reliability-based methodology is presented, which assesses the effect of the load and resistance factors used to design the CRSBF force-controlled members on system-level performance. Next, the adopted building cases, structural modeling and analyses are discussed. Lastly, a case study is presented and the key findings are summarized in the conclusion.

2. Reliability-based design of force-controlled components in controlled rocking steel braced frames

2.1 Overview of the proposed methodology

An overview of the proposed reliability-based methodology is presented in Fig. 1. Relevant aspects of the FEMA P695 guidelines [8] (for assessing collapse performance), the FEMA P58 [9] framework (for assessing post-earthquake structural safety or unsafe placard triggered) and the LRFD component reliability methodology are integrated. The goal is to determine appropriate load (γ) and resistance (ϕ) factors for the beams, columns and braces of the rocking frame that are consistent with the targets set for system level reliability. Assuming a lognormal distribution governs the probabilistic demands and capacities of the braced frame elements, the LRFD methodology describes the relationship between the component reliability index (β), the load and resistance factors and the statistical demand and capacity parameters using the following Eq. (1).

$$\frac{\gamma}{\phi} = \frac{D}{D_n}\frac{C_n}{C} exp\left(\beta\sqrt{\sigma_{lnC}^2 + \sigma_{lnD}^2 - 2\rho\sigma_{lnC}\sigma_{lnD}}\right) \quad (1)$$

D and C_m and D_n and C_n are the median and nominal values of the component demand and capacity, respectively, σ_{lnC} and σ_{lnD} are the lognormal standard deviations and ρ is the correlation between the demand and capacity.

Eq. (1) can be rearranged to compute the β value that corresponds to the γ/ϕ used to design the CRSBF braced frame elements. For a predefined ground motion intensity level, D_m can be obtained from nonlinear response history analyses (NRHAs) using a median structural model that incorporates expected strengths for the yielding elements. D_n is the nominal demand on the rocking frame elements, which is computed based on the maximum expected overturning resistance provided by the PT (F_{pt}) and fuse force (F_f) and the gravity load on the frame (P_D). The equivalent static procedure developed by Steele and Wiebe (2016) [10] is adopted for this purpose.

C $/C_n$ represents the ratio between the median and nominal capacity of the force-controlled elements and is obtained from statistical analysis of experimental data, which is also used to determine the dispersion in the capacity of the force-controlled component (σ_{lnC}). The dispersion in the force-controlled component demand (σ_{lnD}) can include record-to-record (obtained from NRHAs) and other sources (e.g. material strength parameter) of uncertainty. However, only the former is considered in this study. Since the data needed to quantify the correlation between the demand and capacity (ρ) is unavailable, they are assumed uncorrelated.

Having determined the values of the parameters in Eq. (1), β is used to compute the failure probability for the force-controlled component of interest $[P(D > C) = \Phi(-\beta)]$, where $\Phi(\ \ )$ is the standard normal cumulative distribution function. The next step is to compute the probability of exceeding some system-level limit state when the failure of the force-controlled components is included, $P(LS_i|IM)$, (adapted from Victorsson et al. 2011, [11]).

$$P(LS_i|IM) = P\left(LS_{i,Sys}|IM\right) + P\left(LS_{i,D>C}|D > C\right)P(D > C|IM) \quad (2)$$

$P\left(LS_{i,Sys}|IM\right)$ is the probability that limit state i is exceeded conditioned on the intensity level, IM, when the failure of force-controlled components are excluded. $i = 1$ corresponds to an unsafe placard being triggered because of structural damage and $i = 2$ represents collapse. $P\left(LS_{i,D>C}|D > C\right)$ is the probability that limit state i is triggered because of demand exceeding capacity in the force-controlled component and $P(D > C|IM)$ is the probability of demand exceeding capacity in the force-controlled component conditioned on the IM, which is computed using the β value from Eq. (1). The steps needed to generate fragility functions for LS_i and $LS_{i,Sys}$ are detailed later. By integrating these two fragilities with an appropriate hazard curve, the limit state exceedance risks (e.g. probability of collapse in 50 years) with and without consideration given to force-controlled component failure is obtained. The incremental risk added by force-controlled component (in addition to the total risk) is used as the basis for determining the appropriate ϕ/γ to be used in the capacity-design process.

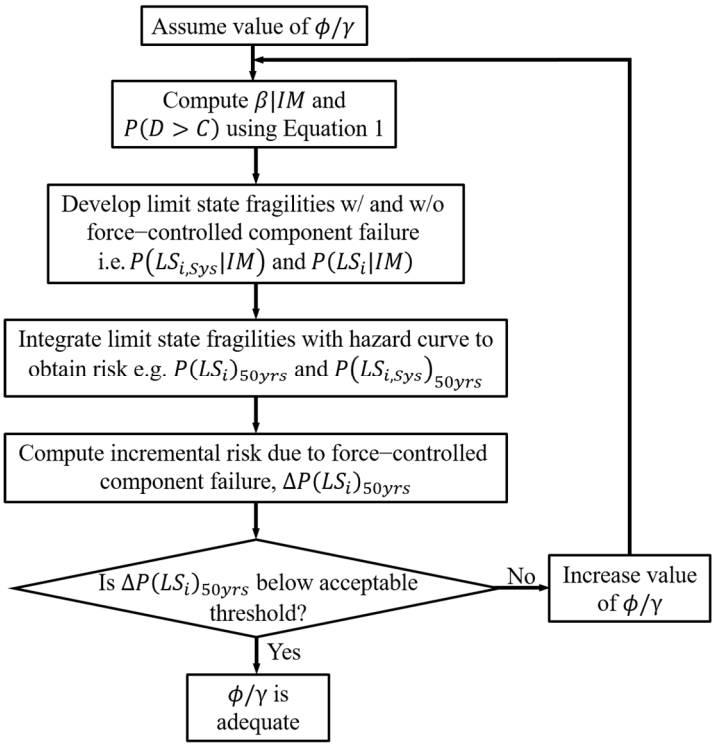

Fig. 1 – Overview of framework for reliability-based determination of load and resistance factors for capacity-designed components of CRSBF

3. Description and design of building cases

3.1 Description of building cases

The reliability-based methodology is applied to 3-, 6- and 9-story CRSBF cases. The three buildings have identical plan dimensions, story heights, gravity loads and framing layout, which are similar to the steel framing configuration used by Gupta and Krawinkler (1999) [12]. All bays are 6.1m wide and the typical story height is 3.96m. The total seismic weights are 13,112kN, 25,868kN and 38,617kN for the 3-, 6- and 9-story buildings, respectively. The 3-story case has two rocking frames in each direction and the 6- and 9-story cases have four. The rocking frames are all located on the perimeter of the building. The frames are configured with

the PT located at the center of the bay. A single shear fuse [2] located mid-bay at the base of the structure is used in each frame for all three building cases.

3.2 Design of building cases

The design loads are based on the ASCE 7-16 [13] standard and the seismicity parameters are taken as $S_S = 1.5$ and $S_1 = 0.6$ with Site Class D (stiff) soil. The designs are based on Risk Category II and Seismic Design Category D with a response modification factor $R = 8$, drift amplification factor $C_D = 5$, and importance factor, $I = 1.0$.

With the exception of the approach used to compute the forces in the beams, columns and braces of the rocking frame, the design procedure presented in Ma et al. (2011) [2] is adopted. The number and size of the PT strands are selected such that they will remain elastic for an uplift ratio corresponding to the drift limit at the maximum considered earthquake (MCE) hazard level, $\theta_{MCE} = 2.5\%$. The effective width of the fuse is determined such that the shear deformation demand corresponding to θ_{MCE} does not exceed 20% [2]. The design drifts are estimated using the iterative approach developed by Ma et al (2011) [2]. The equivalent static procedure developed by Steele and Wiebe (2016) [10] is used to compute the design forces for the beams, columns and braces of the rocking frame.

4. Structural modeling, seismic hazard and ground motions

4.1 Structural modeling

Two-dimensional nonlinear structural models are developed in OpenSees for the three building cases. A schematic representation of the numerical model for the 3-story building case is shown in Fig. 2. To evaluate the effect of force-controlled component failure on system level performance, four sets of models are needed for each building case. For one of the models, the inelastic behavior of the three force-controlled components is excluded ("All-Elastic" in Table 1). This model uses linear elastic beam-column elements for the braces, beams and columns. The other models are developed to consider the inelastic response for each type of force-controlled element. The combinations of inelastic versus elastic rocking frame components used in each type of model is summarized in Table 1. The models identified as "Brace-NL", "Beam-NL", and "Column-NL" only consider material nonlinearity in braces, beams, and columns respectively. For the "All-Inelastic" model, material nonlinearity is incorporated in all three force-controlled elements.

For the models where their inelastic response is considered, the beams, columns, and braces are represented using fiber cross sections that incorporate the Giufrré–Menegotto–Pinto material model with 0.3% strain hardening and expected strengths of $R_y F_y$ $\left(R_y = 1.1 \text{ and } F_y = 308.2\ N/mm^2\right)$. Brace buckling is captured by incorporating corotational transformations and initial imperfections. The discretization of the brace elements along the length and the numbers of fibers and integration points are based on the recommendations by Uriz et al. (2008) [14]. Brace fracture resulting from low-cycle fatigue is captured using the model by Uriz (2005) [15]. Pinned connections are used at the end of the braces and beam-column connections and rigid elastic elements are placed in the region of the gusset plate at the ends of the beams, columns and braces.

The PT strands are modeled using corotational trusses with hook elements (tension only) and a multilinear material to capture initial and complete fracture [2]. The expected yield stress $\left(f_{y,f}\right)$, initial fracture stress $\left(f_{u,f}\right)$ and elastic modulus of the PT material are 1657.4 N/mm^2, 1861.6 N/mm^2 and 195 KN/mm^2, respectively. The corresponding yield $\left(\epsilon_{y,f}\right)$ and initial fracture $\left(\epsilon_{u,f}\right)$ strains are 0.87% and 1%, respectively. Upon initial fracture, the PT degrades to zero stress at a strain value of 5%. The behavior of the energy-dissipating fuses is represented using the assembly model proposed by Ma et al. (2011) [2], which includes a truss element to capture axial stiffness and a beam element with large flexural stiffness and rotational

springs on each end. Expected strengths of R_yF_y $(R_y = 1.1$ and $F_y = 308.2\ N/mm^2)$ are also used for the fuse material. The expected yield strength and initial stiffness of the fuse is calculated based on its geometric properties. The shear deformation at initial and ultimate fuse fracture (zero stress) are $\gamma_u = 0.35$ and $\gamma_m = 0.5$, respectively. The post yield stiffness of the fuse is taken to be 4% of the initial stiffness [2].

Rocking behavior is simulated using compression-only gap elements placed at the base of each column. These gap elements have zero tensile stiffness and are near-rigid in compression. Rayleigh damping is used with 2% of critical damping applied to the first and third modes. A leaning column is placed on each side of the rocking frame to capture the destabilizing effect of gravity loads on frames not included in the structural model. Pin-ended strut elements are used to connect the rocking frame to the leaning columns.

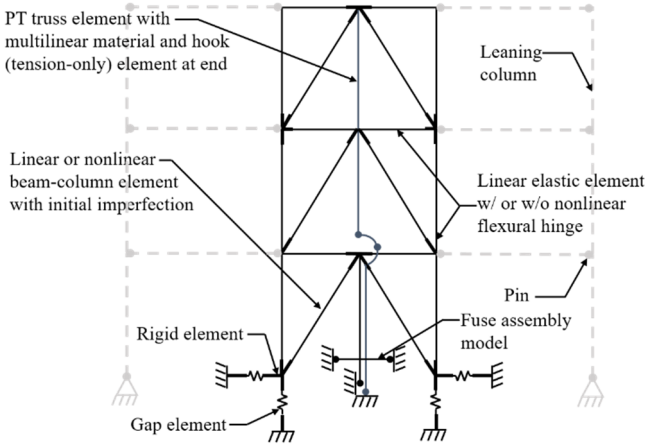

Fig. 2 – Schematic representation of the numerical model for the 3-story CRSBF

Table 1 – Summary of model cases with and without consideration of inelastic response in force-controlled components

Model ID	Braces				Beams		Columns	
	Elastic Elements	Nonlinear Elements	Initial Imperfection	Fracture Considered	Elastic Elements	Nonlinear Elements	Elastic Elements	Nonlinear Elements
All-Elastic	√	x	x	x	√	x	√	x
All-Inelastic	x	√	√	√	x	√	x	√
Brace-NL	x	√	√	√	√	x	√	x
Beam-NL	√	x	x	x	x	√	√	x
Column-NL	√	x	x	x	√	x	x	√

√: Included in model
x: Not included in model

4.2 Seismic hazard, ground motions and nonlinear response history analyses

The results from nonlinear response history analyses are to compute the reliability index (more specifically, D) for the force-controlled components (Eq. (1)) and the system-level limit state fragility functions (Eq. (2)). The forty-four (twenty-two pairs) far-field ground motions specified in the FEMA P695 [8] guidelines are used for this purpose. The spectral acceleration corresponding to the first mode period (Sa_{T1}) is used as the ground motion intensity measure (IM).

To support a risk-based assessment of the impact of force-controlled component failure on system performance, a site-specific hazard curve is incorporated based on Sa_{T1}. The hazard curve corresponding to the first-mode periods of the three building cases is used for a Los Angeles site (33.58, -118.19).

5. Application of reliability-based capacity design methodology

This section applies the reliability-based methodology to the three building cases. As previously noted, the outcome is a quantitative relationship between ϕ/γ and the system-level vulnerability and risk-based performance. Initially, the procedure is described and intermediate results are presented for the case where $\phi/\gamma = 0.9$ ($\phi = 0.9$, $\gamma = 1$) and $\rho = 0$. The results for a range of ϕ/γ values are summarized and discussed and the implications of non-zero ρ values are also examined. The value of γ reflects the hazard-level that is used to determine the design forces for the force-controlled components. In prior studies (e.g., [1, 2, 10]), the MCE hazard level has been used as the default and is therefore associated with $\gamma = 1$ herein. The γ value for other hazard levels is taken as the ratio between the corresponding Sa_{T1} and S_{MT}. Since ϕ is structural-system-agnostic and assessed based on a broad set of considerations not explicitly related to CRBFs, it is assumed that a value of 0.9 will always be used. Therefore, the target ϕ/γ will be achieved by considering γ as the variable parameter. In other words, the hazard level used to determine the force-controlled component design forces will be the control factor that is used to achieve the desired ϕ/γ value.

5.1 Computing β and P(D > C)

The value of β and $P(D > C)$ corresponding to $\phi/\gamma = 0.9$ is computed for a range of intensity levels. For this purpose, incremental dynamic analyses (IDAs) are performed using the structural model where the inelastic response of the force-controlled components is not included ("All Elastic" in Table 1). In other words, the beams, columns and braces of the rocking frame are modeled using linear elastic elements. Using the results from the set of forty-four ground motions, the median (D_m) and log-standard deviation (σ_{lnD}) of the demand in each type of element is computed. C_m/C_n is taken as 1.87 [16] and σ_{lnC} is taken as 0.15 [11] for the axial capacity of the members. D_n is computed using the Steele and Wiebe (2016) [10] methodology described earlier.

Eq. (1) is used to compute the value of β conditioned on the intensity-level and component type. The β values are then used to obtain $P(D > C)$ using the following relationship: $P(D > C) = \Phi(-\beta)$. Fig. 3 shows plots of the maximum-value envelope (i.e. maximum value at each intensity considering all elements in all stories) of $P(D > C)$ versus Sa_{T1} normalized by the S_{MT}, for the axial force in the braces, beams and columns. For the 3-,6-, and 9- story buildings, $P(D > C)$ is generally highest in the beams and braces. For the latter, the MCE level $P(D > C)$ is 0.38, 0.37 and 0.34 for the 3-, 6- and 9-story building, respectively. At the same intensity, the $P(D > C)$ values in the beams are 81% of the brace values. The columns have the lowest $P(D > C)$ with MCE level values of 0.036, 0.044 and 0.028 for the 3-, 6- and 9-story buildings, respectively. The lower $P(D > C)$ values in the columns relative to the beams and braces is explained by comparing the dispersion in the force demands in the three components which is one of the inputs in Eq. (1). More specifically, the dispersion in the column force demands (σ_{lnD}) is approximately 30% that of the beams and braces at the MCE level.

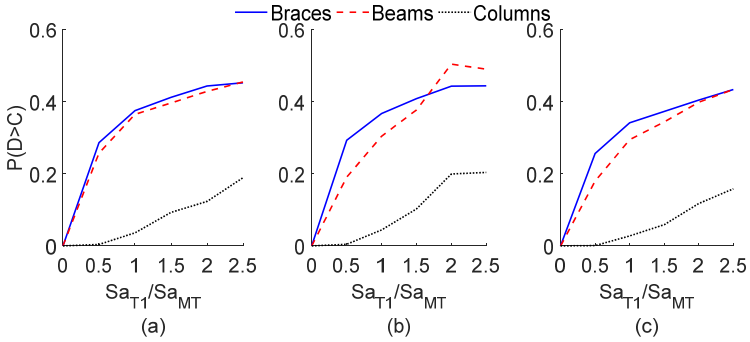

Fig. 3 – Maximum of $P(D > C)$ versus Sa_{T1}/Sa_{MT} corresponding to axial forces in force-controlled components (a) 3-, (b) 6- and (c) 9-story building cases

5.2 Impact of force-controlled component failure on system-level performance

The impact of force-controlled component behavior on the CRSBF system-level performance is quantified by computing the incremental risk caused by failure of the rocking frame beams, columns and braces. The first step in this sub-process is to develop limit state fragility functions with and without considering failure in each component. Collapse and post-earthquake structural safety (or unsafe placard triggered by structural damage) are the two system-level limit states considered. The expectation is that the CRSBF capacity-design criteria will be different for the two limit states. More specifically, if the same acceptable risk-threshold is assumed, the required ϕ/γ is expected to be smaller (i.e. a more conservative design) for the unsafe placard limit state.

5.2.1 Collapse safety

Collapse fragility functions are developed without considering force-controlled component failure $\left[\text{i.e. } P\left(Collapse_{Sys}|IM\right)\right]$ using the same structural model (All-Elastic) and IDA results described earlier. Fig. 4 shows the fragility curve obtained from the All-Elastic model for the three building cases after incorporating SSF and β_{TOT}. The intensity levels on the horizontal axis are normalized by the S_{MT}. The 3-, 6-, and 9-story buildings have adjusted collapse margin ratios $\left(\text{CMR}_{Sys}\right)$ of 3.1, 4.5, 5.0 respectively.

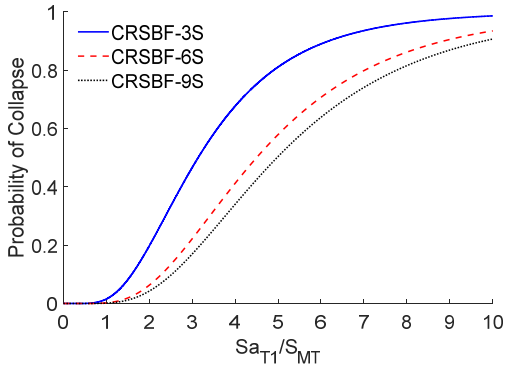

Figure 4 – Collapse fragility curves for "All-Elastic" 3-, 6- and 9 story buildings cases i.e. force-controlled component failure not considered

Multiple numerical models and analysis cases are needed to compute the incremental collapse fragility caused by force-controlled-component-failure $\left[\text{i.e. } P(Collapse_{D>C}|D>C)P(D>C|IM)\right]$. A different structural model is needed for each type of component and loading mechanism. For instance, to assess the relationship between brace ϕ/γ and collapse performance, the All-Elastic and Brace-NL models (Table 1) are used. Using the All-Elastic model, $P(D>C|IM)$ at each intensity level is obtained from the results shown in Fig. 3. From these same analyses, the ground motions that do not cause collapse but the brace axial force demand exceeds the nominal capacity are identified. Denoted as $\left[GMs_{D>C,\overline{Collapse}}|IM\right]$, this subset of ground motions is used to perform IDAs on the Brace-NL model. At each intensity level, $P(Collapse_{D>C}|D>C)$ is computed as the fraction of collapse cases relative to the $\left[GMs_{D>C,\overline{Collapse}}|IM\right]$ record-set. Finally, the incremental collapse fragility caused by brace axial failure is computed as $P(Collapse_{D>C}|D>C)P(D>C|IM)$. This process is repeated using Beam-NL and Column-NL, which consider axial failure in the beams and columns. Fig. 5 shows collapse fragility curves for all three building cases with and without considering beam, column and brace failure.

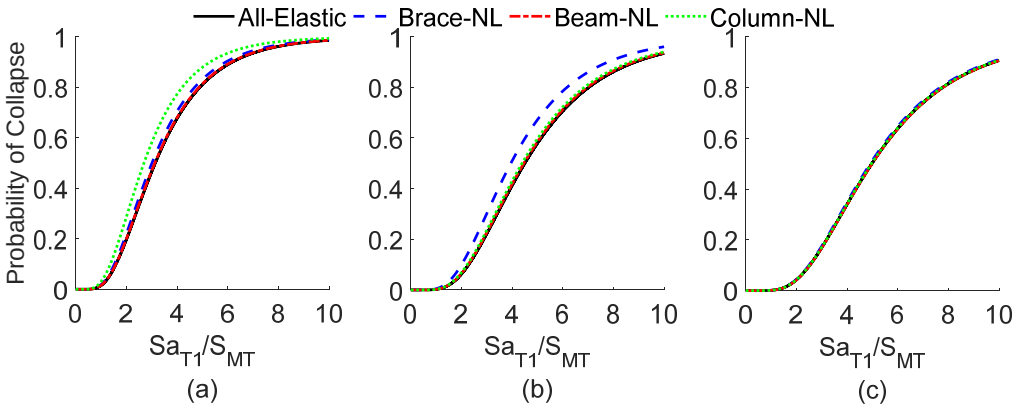

Fig. 5 – Collapse fragility curves with and without consideration of force-controlled component failure for the (a) 3-, (b) 6- and (c) 9-story building cases

5.2.2 Unsafe Placard Triggered by Structural Damage (Post-Earthquake Structural Safety)

In addition to collapse, we also examine the effect of ϕ/γ on the probability that an unsafe placard is assigned to the building because of structural damage. The framework developed by FEMA P58 [9] is adopted for this purpose.

Note that FEMA P58 groups the elements of a braced frame to define the UPT. In other words, the damage state descriptions and triggering ratios are defined for the entire frame and not the individual elements (beams, columns and braces). Therefore, unlike the collapse limit state, the relationship between ϕ/γ and the likelihood of an unsafe placard being assigned is established for the entire frame (as opposed to the individual elements). In addition to the force-controlled braced frame elements, the PT strands and fuse are also considered as UPT components. The damage state IDs, descriptions, median and dispersion of the associated EDP limits and triggering ratios for each UPT-component are summarized in Table 2. The EDP limits and triggering ratio for the braced frame are from the FEMA P58 guideline. PT yielding and the onset of strength degradation in the fuse are adopted as UPTs assuming the deterministic EDP limits specified earlier.

Like the collapse limit state, the unsafe placard fragility function without the consideration of force-controlled component failure $\left[\text{i. e. } P\left(Unsafe_{Sys}|IM\right)\right]$ is generated using the analysis results from the ALL-Elastic model. The force-controlled components are excluded as UPTs in this assessment case.

The unsafe placard fragility caused by force-controlled component failure is directly computed. In other words, instead of computing $P(Unsafe_{D>C}|D>C)P(D>C|IM)$ and adding it to $P\left(Unsafe_{Sys}|IM\right)$ (as was done the collapse limit state), $P(Unsafe|IM)$ is obtained directly by applying the assessment process incorporating the grouped force-controlled components as a UPT. For instance, to compute $P(Unsafe|IM)$, the EDPs produced from IDAs on the All-Inelastic model are utilized. Building damage realizations are then generated incorporating braced frame failure as a UPT (in addition to the deformation-controlled components). To perform IDAs, ground motions are scaled until an unsafe placard is triggered for at least half of the ground motions. Unsafe placard fragility functions developed with and without considering all force-controlled components, are shown in Fig. 6 for the three buildings. As expected, the median intensity level associated with the UPT limit state is much lower (by factors ranging from 2.5 to 2.7) than for collapse. However, Fig. 6 shows that force-controlled component failure has a negligible effect on the UPT limit state for all three building cases. The lower intensity levels associated with the UPT limit state (compared to collapse) and the generally low $P(D>C)$ values shown in Fig. 6 (even up to the MCE hazard level) explains the negligible effect of force-controlled component failure observed in Fig. 6. In other words, the capacity-design procedure that is implemented for the braced frame components minimizes their potential influence on the UPT limit state.

Table 2 – UPT-components, damage states, EDP limits and triggering ratios

Element	Damage State			EDP Limit		
	ID	Description	Triggering Ratio/Value	Type	Median	Dispersion
Forced- controlled elements i.e. beams, columns and braces	FC-DS-1	Initiation of brace bucking and yielding of gusset plates.	NA[1]	Story Drift Ratio	0.00159	0.7
	FC-DS-2	Brace buckling.	0.4		0.01	0.3
	FC-DS-3	Fracturing of braces and bolts of beam-column connections. Torn gusset plates, and local buckling of frame members.	0.2		0.0178	0.3
PT	PT-DS-1	Yielding of PT strands	1.0	Strain	0.0086	NC[2]
Fuse	FS-DS-1	Onset of strength degradation in fuse	1.0	Shear Def.	0.35	NC

[1]NA: Damage state cannot trigger an unsafe placard

[2]NC: Disperion not considered

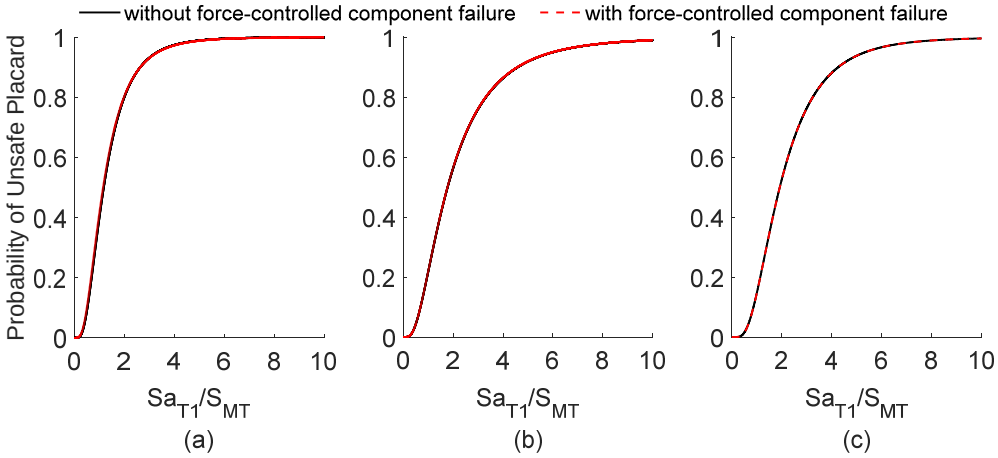

Fig. 6 – Unsafe placard fragility curves with and without the consideration of force-controlled component failure for (a) 3-, (b) 6- and (c) 9-story building cases

6. Risk-based assessment of the impact of force-controlled component failure on system-level performance

The load and resistance factors for the force-controlled components are determined based on the extent to which they contribute to the risk of limit-state (collapse and unsafe placard) exceedance over the service-life of the CRSBF building. Fig. 7 shows how each type of force-controlled component affects the 50-year probability of collapse over a range of ϕ/γ values where $\frac{\phi}{\gamma} = 0$ corresponds to the case where force-controlled component failure is not considered and $\frac{\phi}{\gamma} = 0.9$ is the value that is the basis of current design standards (i.e. [13, 17]).

As expected, the collapse risk generally increases with the value of ϕ/γ. Recall that higher values of ϕ/γ corresponds to lower γ values and hazard levels (less conservative force-controlled component design). For 3-story building, column failure has a significant effect on collapse risk, which is consistent with Fig. 5. For 6-, and 9-story buildings beam failure has a modest effect on collapse risk at higher $\frac{\phi}{\gamma}$ values. As indicated earlier, taller buildings are more susceptible to P-Δ-triggered or sidesway collapse compared to shorter buildings, which reduces the overall influence of force-controlled component failure for this limit state. The 50-year collapse risk for all three cases remains below the 1% threshold that is implied in modern design codes and standards (e.g. [13]).

The effect of ϕ/γ on the probability that the CRSBF building is assigned an unsafe placard within a 50-year period is shown in Fig. 8. Similar to Fig. 7, $\phi/\gamma = 0$ corresponds to the case where force-controlled component failure is not considered and the return period corresponding to each ϕ/γ is shown in the upper horizontal axis. When force-controlled component failure is not considered, the 50-year probability of an unsafe placard is 3.1%, 1.5% and 1.1% in the 3-, 6- and 9-story building cases, respectively. For the 3-story building, there is a dramatic increase in the effect of force-controlled component failure on the 50-year probability of an unsafe placard between ϕ/γ values of 1.2 and 1.8. However, for the taller building cases, there is not an appreciable change in the effect of force-controlled component failure on the UPT limit state as ϕ/γ increases. The triggering effect of the PT and fuse "masks" that of the force-controlled components for the UPT limit state. Moreover, because the shorter buildings are dominated by first mode (or rigid-body-rotation) behavior, the increasingly nonlinear response caused by force-controlled component failure leads to higher roof drift demands, PT strains and fuse deformations. In contrast, because of the greater contribution of higher modes in taller buildings, while force-controlled component nonlinearity leads to higher story drifts, the effect on roof drift demands, PT strains and fuse deformations is smaller.

The 50-year probability of an unsafe placard when $\frac{\phi}{\gamma} = 0.9$ (the value implied by the current design codes and standards) is 3.5%, 1.5% and 1.1% for the 3-, 6- and 9-story building cases, respectively. Note that, unlike collapse, current design codes and standards do not consider the risk of an unsafe placard and therefore no limit is provided. However, given that the CRSBF is being developed as a high-performance seismic system, this limit state should be given high priority when developing design guidelines.

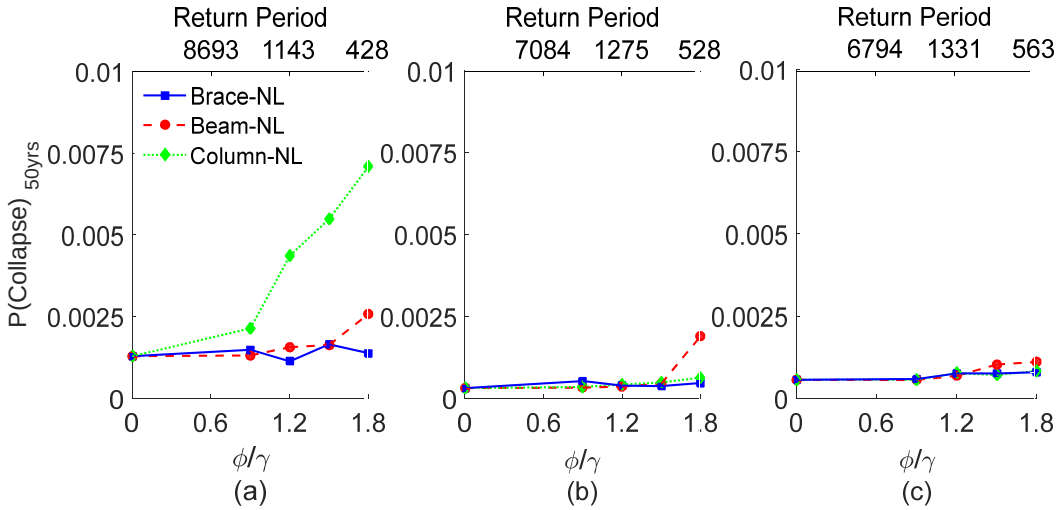

Fig. 7 – Effect of ϕ/γ (and corresponding return period) on the probability of collapse in 50 years for the (a) 3-, (b) 6- and (c) 9-story building cases

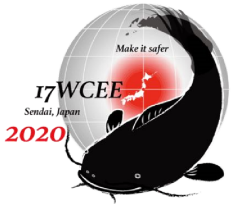

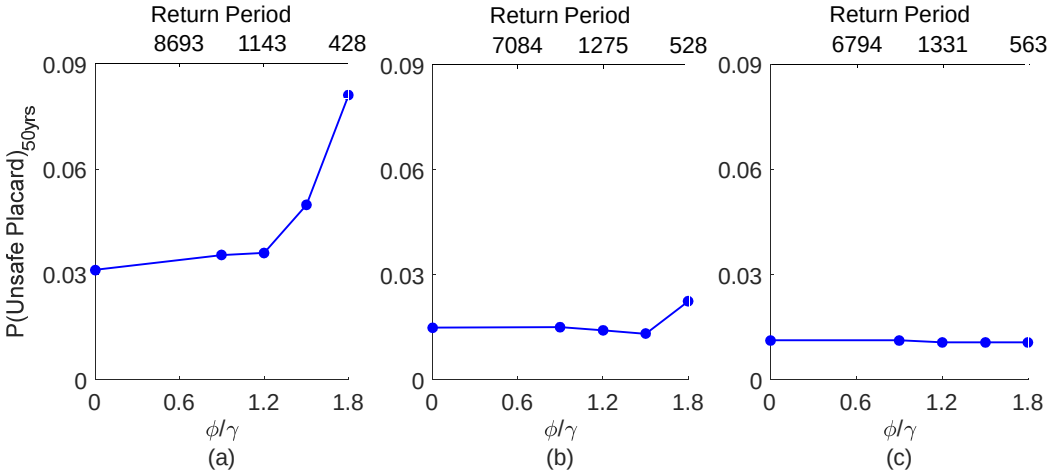

Fig. 8 – Effect of ϕ/γ (and the corresponding return period) on the probability of an unsafe placard being assigned within a 50-year period for the (a) 3-, (b) 6- and (c) 9-story building cases

7. Summary and conclusion

A reliability-based approach to designing CRSBF force-controlled components (i.e. frame beams, columns and braces) is presented. Central to the proposed methodology is establishing an explicit link between the failure of these components and the CRSBF system-level performance. Collapse and post-earthquake structural safety (or unsafe placard assignment) are the two considered system-level limit states. A case study is presented whereby the newly developed methodology is applied to 3-, 6- and 9-story building cases.

The effect of frame beam, column and brace failure on the vulnerability to collapse and unsafe placard triggering (UPT) was first assessed for a resistance and load factor ratio of $\frac{\phi}{\gamma} = 0.9$ (the value implied by current standards). The ratio of adjusted collapse margin ratio (CMR) with and without considering force-controlled component failure ranged from 0.86 to 1.0 at $\frac{\phi}{\gamma} = 0.9$, while the same ratio for the UPT limit state ranged from0.98 to 1.0. Furthermore, a disaggregation of the UPT vulnerability showed that the deformation-controlled components (fuse and PT) were much more likely to trigger an unsafe placard compared to the force-controlled components. For both limit states, the effect of force-controlled component failure was found to be lower for taller buildings.

A risk-based assessment of the effect of force-controlled component failure was conducted for $\frac{\phi}{\gamma}$ =0.9, 1.2, 1.5 and 1.8 was also performed.

8. Acknowledgements

This research is supported by National Science Foundation Award No. 1554714.

9. References

[1] Eatherton M and Hajjar J (2010): Large-scale cyclic and hybrid simulation testing and development of a controlled-rocking steel building system with replaceable fuses. NSEL-025, Department of Civil and Environmental Engineering, University of Illinois at Urbana-Champaign.

[2] Ma X, Krawinkler H, and Deierlein GG (2011): Seismic design and behavior of self-centering braced frame with controlled rocking and energy dissipating fuses. John Blume Earthquake Engineering Center, TR 174, Stanford, CA.

[3] Hall KS, Eatherton MR, and Hajjar JF (2010): Nonlinear behavior of controlled rocking steel-framed building systems with replaceable energy dissipating fuses. Newmark Structural Engineering Laboratory. University of Illinois at Urbana-Champaign.

[4] Eatherton M, and Hajjar J (2011): Residual drifts of self-centering systems including effects of ambient building resistance. *Earthquake Spectra*, 27(3), 719–744.

[5] Eatherton M, Ma X, and Krawinkler H. et al (2014): Design concepts for controlled rocking of self-centering steel-braced frames. *J. Struct. Eng.*, 140:4014082.

[6] Wiebe L, and Christopoulos C (2014a): Performance-based seismic design of controlled rocking steel braced frames. II: Design of capacity-protected elements. *J. Struct. Eng*., 141 (2014) 04014227.

[7] Wiebe L, and Christopoulos C (2014b): Performance-based seismic design of controlled rocking steel braced frames. I: Methodological framework and design of base rocking joint. *J. Struct. Eng.*, 141(9):040142261–10.

[8] FEMA (Federal Emergency Management Agency) (2009) Quantification of building seismic performance factors, FEMA P695. Redwood City, CA

[9] FEMA (Federal Emergency Management Agency) (2012) Seismic performance assessment of buildings. FEMA P-58, Volumes 1 and 2. Redwood City, CA

[10] Steele TC, and Wiebe L. (2016): Dynamic and equivalent static procedures for capacity design of controlled rocking steel braced frames. *Earthquake Engng Struct. Dyn*. DOI: 10.1002/eqe.2765

[11] Victorsson, VK, Deierlein GG, Baker JW, and Krawinkler H (2011): The Reliability of Capacity-Designed Components in Seismic Resistant Systems. *J.A. Blume Technical Report* 177, Stanford University, Stanford, CA.

[12] Gupta A, and Krawinkler H (1999): Seismic demands for the performance evaluation of steel moment resisting frame structures. Stanford University, Stanford, CA

[13] ASCE/SEI. (2016). *Minimum design loads and associated criteria for buildings and other structures ASCE/SEI 7-16*. Reston, VA.

[14] Uriz P, Filippou FC, and Mahin SA (2008): Model for Cyclic Inelastic Buckling of Steel Braces. *J. Struct. Eng* 134(4).

[15] Uriz P (2005): Towards earthquake resistant design of concentrically braced steel structures." Ph.D. dissertation, Dept. of Civil and Environmental Engineering, Univ. of California, Berkeley, CA.

[16] Fell BV, Kanvinde AM, Deierlein GG, Myers AT, and Fu X (2006): Buckling and fracture of concentric braces under inelastic cyclic loading. *SteelTips Series*, Structural Steel Education Council, Moraga, CA.

[17] AISC (2016). *American Institute of Steel Construction Manual*. Fifteenth Edition, American Institute of Steel Construction, United States of America.